

Using $\gamma\gamma$ -Coincidence Spectroscopy to Identify Natural Radiation in Soils Near the Mississippi River

Pranjal Singh,^{1, a)} Daniel Valmassei,¹ Anthony Kuchera,¹ and Ben Crider²

¹⁾*Department of Physics, Davidson College, Davidson, North Carolina 28035, USA*

²⁾*Department of Physics and Astronomy, Mississippi State University, Mississippi State, Mississippi 39762, USA*

^{a)}*Corresponding author: prsingh@davidson.edu*

Abstract. Naturally radioactive nuclides present in soils contain background radiation that humans are exposed to every day. Previous research suggests that there are high background radiation areas (HBRAs) caused by climate, geography, wind, and water currents that accumulate a higher concentration of these radionuclides. An investigation of the Nile Delta confirms the presence of minerals rich in U and Th from monazite and zircon, further suggesting that certain locations have a higher concentration of these radionuclides. The present work is a search for monazite in Great River Road State Park, near the Mississippi River. The acquired samples were measured with a low-background NaI(Tl) spectrometer and digital data acquisition system. Using $\gamma\gamma$ -coincidence spectroscopy to reduce background radiation, we were able to apply coincidence gates of known gamma-ray energies originating from ^{238}U and ^{232}Th decay chains to identify the presence of the radionuclides in the soil samples. From our results, we confirmed that there is an accumulation of minerals containing ^{238}U and ^{232}Th near the river. Our next steps will focus on calculating activities for quantitative results and collecting samples from an extended region along the river.

INTRODUCTION

Water and air currents dictate accumulation of minerals around the shores of rivers, which results in a nonuniform spread of minerals containing naturally radioactive nuclides that contribute to the outdoor terrestrial natural radiation. Most soils have some amount of natural radionuclides such as ^{40}K , ^{238}U , ^{235}U , and ^{232}Th , that humans are exposed to every day.¹ A previous study by Mubarak et al. determined the Nile Delta near Rosetta Beach in Egypt to be a high background radiation area (HBRA) for deposits of beach placer or "black sand," which contains concentrations of monazite and zircon minerals along with a few others.¹ Monazite is a rare earth element mineral. Due to its high resistance to weathering, it can mostly be found in sedimentary matter and is valued for its thorium content.² The monazite that we are concerned with is fluvial monazite, found in rivers. Monazite has the highest concentration at the lower levels of the matter left behind by a river (alluvium), but some of it can continue downstream. If this alluvium contains gravel, then the monazite can get trapped between the spaces in the gravel; however, in many cases most of the monazite contributes downstream.³

As per geological reports, the largest concentrations of radioactive nuclides near the Mississippi Gulf Coast and associated offshore islands are found in the beach sands, with monazite being the most frequent mineral found.⁴ The attributes of monazite are indicative of a formation in metamorphic rocks and the grade of metamorphism governs the concentration of thorium in the mineral,⁵ but it is also said to contain a presence of uranium. This study investigates the formation of radionuclides in soil of Great River Road State Park, near the Mississippi River, for an exploration into the presence of monazite.

EQUIPMENT AND METHODS

The setup for this investigation used two NaI(Tl) detectors (Scionix model 152AS102/5M-E2-X) each consisting of a cylindrical NaI(Tl) scintillation crystal with a diameter and height of 152 mm and 102 mm, respectively, with a stainless steel housing. The crystals were coupled with a low-background ET9390 photomultiplier tube (PMT), 127 mm in diameter, and a quartz optical window, to yield a low background radiation. The detectors faced each other at a distance of 8 cm and were enclosed by lead to reduce background radiation, as seen in Fig. 1 and Fig. 2. The enclosure consists of six 2-inch-thick lead bricks on the front and back and a lead 0.75-inch-thick slab on the top and bottom.

The detectors were biased with voltages of approximately 700 V and a preamplifier which was powered by +5 V. The data acquisition and processing system was XIA Pixie-Net, a multichannel digital spectrometer designed for high-precision coincidence spectroscopy by detector signal digitization, waveform capture, pulse height measurement, time stamping, online pulse shape analysis with 12-bit resolution, and 250 Megasamples per second pulse processor. The Pixie-Net software is managed by a collection of C/C++ programs. All collected data was analysed using the ROOT data analysis framework to obtain the presented histograms.⁶

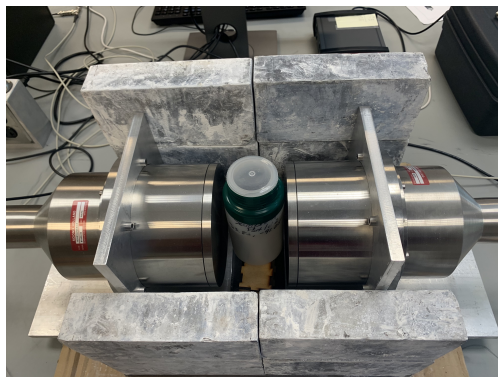


FIGURE 1: Two NaI(Tl) detectors placed 8 cm apart with a sample.

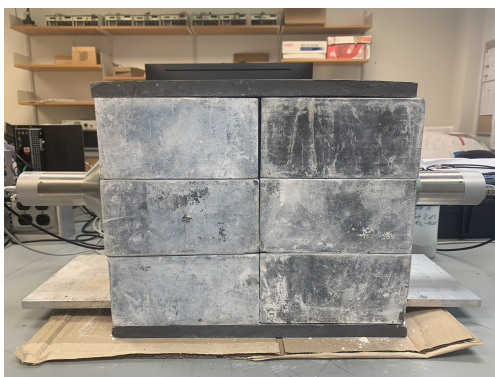


FIGURE 2: Lead enclosure of the detectors for low-background counting setup.

Five calibration sources (^{137}Cs , ^{60}Co , ^{57}Co , ^{54}Mn , ^{22}Na) were used for the conversion from multichannel analyzer (MCA) spectrum to energy. Each calibration source was measured for 5 minutes, and their MCA values were extracted by fitting the peaks with Gaussian distributions using ROOT to calculate a slope and offset from known gamma-ray energies. The energy resolution of each of the detectors, determined using the full width at half maximum divided by the actual value (661.7 keV) of ^{137}Cs , was approximately 7%.

Two sets of soil samples (samples A and B) were collected in a few steps proximity of each other at a location off the trails in the Great River Road State Park. The exact location can be seen in Fig. 3. After collection the samples were dried and sealed in plastic bottles, see Fig. 1. Data for each sample was collected for 24 hours. The laboratory background, with no sample and bottle, was also measured for the same duration.

Coincidence spectroscopy was used to reduce background radiation further and identify the nuclides in the samples. To confirm the presence of ^{232}Th and ^{238}U , we applied coincidence gates from a study by Tillett et al.,⁷ where coincidence gates represent the energy of a specific state into which other excited states transition. The coincidence gates for ^{232}Th and ^{238}U are extracted from the β decays of ^{208}Tl to ^{208}Pb and ^{214}Bi to ^{214}Po , respectively, which can be seen in Fig. 4. It is important to note that ^{208}Tl and ^{214}Bi are not direct byproducts of ^{232}Th and ^{238}U but are products after numerous α and β decays. The γ rays originate from the transition of the first excited state to the ground state, where there are multiple transitions feeding into the first excited state by higher states from the β decays. Figures 5 and 6 present all events that fall within the 500-ns coincidence window. This coincidence window was applied in software to only keep events in which both detectors measured gamma rays. The energy gate is applied to one detector, then a 1-D histogram of all events from the other detector that come in coincidence with that gate is plotted to identify the radionuclide. To ensure that our detector is able to measure ^{232}Th and ^{238}U and to make certain that the known coincidence gates (2614 keV and 609 keV) provide the expected results, we tested samples known to contain ^{232}Th and ^{238}U . Our results reflected similar findings to Tillett et al. of activities of thorium and uranium in environmental samples. With this method verified, we applied the same approach to the soil samples.⁷



FIGURE 3: Map of Great River Road State Park with marker at (33°49'48.0"N, 91°03'00.0"W) where samples were taken.

RESULTS

The 2-D histograms shown in Figs. 5 and 6 present all events in coincidence from both detectors. For coincidence gating, we looked specifically for vertical bands, indicating a particular energy in one detector; the diagonal bands represent Compton scattering and any other events in which an incident gamma ray deposits some of its energy into one detector and the remaining in the other. By referencing a background 2-D coincidence histogram, we were able to determine that the vertical band closer to 500 keV is seen consistently in all data. The 609-keV and 2614-keV gates presented in the 2-D histograms are not present in the background and correspond to the ^{238}U and ^{232}Th , respectively.

The gates restrict allowed energy values from one axis and project the allowed counts onto the other, producing 1-D histograms that only show events that come in coincidence with the energy gate of the other detector. Figures 7 and 8 are 1-D projections of the 609-keV ^{238}U energy gate. We are able to identify some of the gamma rays from ^{214}Po , a product of the decay chain of ^{238}U , and in comparison to the histograms in a study by Tillett *et al.*⁷ The corresponding energy values are comparable to the transition energies from higher to the first excited state of ^{214}Po . Lower energies are unable to be distinguished from Compton scattered gamma rays, as they overlap at the same energies and have weak transition probabilities of only 5% and 3%.

Figures 9 and 10 are 1-D projections of the 2614 keV energy gate that corresponds to ^{232}Th . The relative intensity and shape of the peaks are comparable to the the histograms in the study by Tillett *et al.*⁷ for ^{232}Th , and the measured values also yield the transition energy values from higher states to the first excited state of ^{208}Pb .

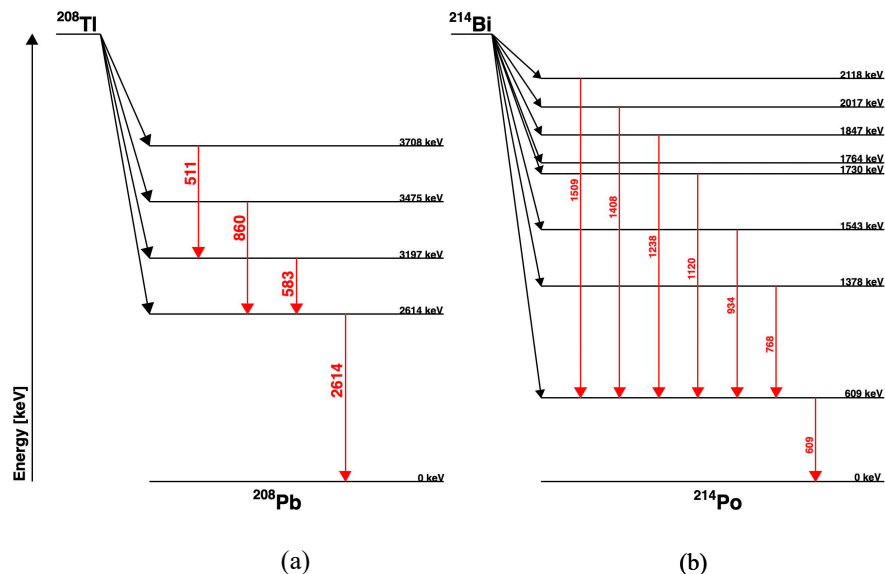


FIGURE 4: ^{208}Tl to ^{208}Pb (a) and ^{214}Bi to ^{214}Po (b) transitions show the origination of expected gamma energies from the parent nuclei ^{232}Th and ^{238}U .

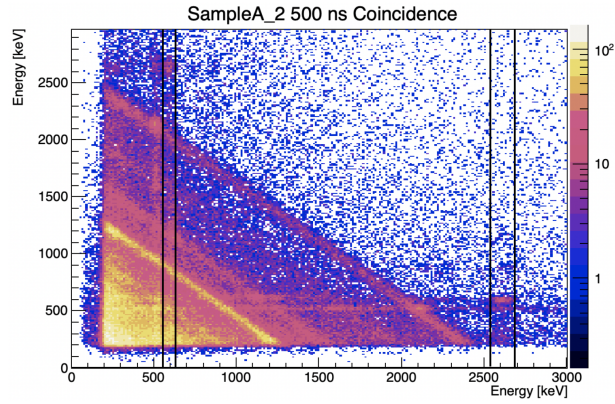


FIGURE 5: Sample A 2-D coincidence histogram with coincidence gates of ²³⁸U (609 keV) and ²³²Th (2614 keV), shown by vertical black lines.

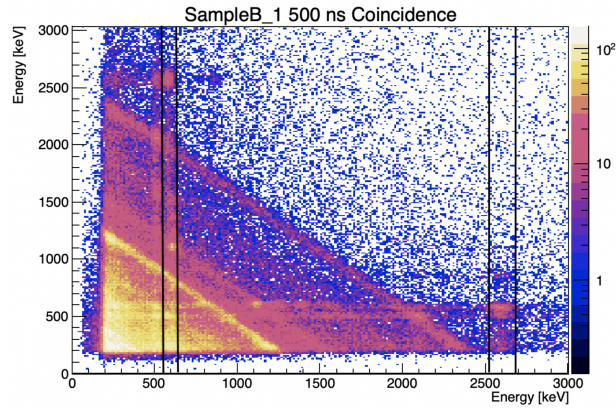


FIGURE 6: Sample B 2-D coincidence histogram with coincidence gates of ²³⁸U (609 keV) and ²³²Th (2614 keV), shown by vertical black lines.

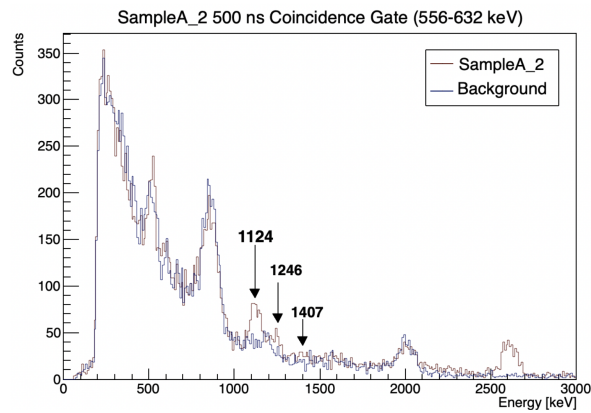


FIGURE 7: Sample A 1-D projection to Y-axis of the ²³⁸U (609 keV) coincidence gate. The labeled peaks correspond to transitions from Fig. 4 (²¹⁴Po).

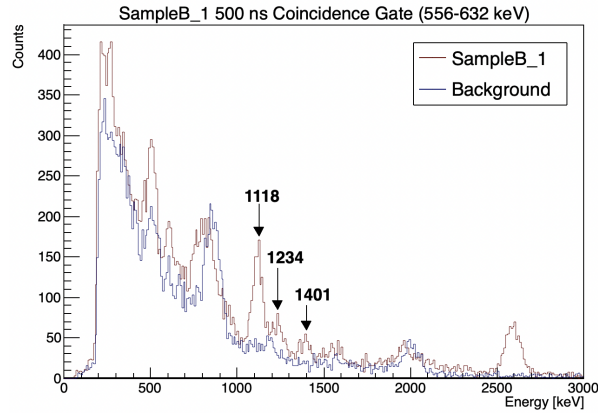


FIGURE 8. Sample B 1-D projection to Y-axis of the ^{238}U (609 keV) coincidence gate. The labeled peaks correspond to transitions from Fig. 4 (^{214}Po).

CONCLUSIONS

The 1-D histograms produced by the energy coincidence gate method allowed us to crossreference with known transition energies of gamma rays emitted by nuclei in the decay chains of ^{232}Th and ^{238}U to determine the present radionuclides.

Upon confirming the presence of ^{232}Th and ^{238}U , next steps include improving our understanding of our detector efficiencies so that we can quantify the activities of the radionuclides in the soil samples. Additionally, we would also need accurate measurements of the masses of the samples without the bottle.

The measured peaks from the 1-D gated coincidence plots for sample B have more counts than sample A. As the run times for both samples are the same, this variance can point to a difference in activity of the radionuclides. The study by Mubarak et al. collected 12 samples with a spacing of 600 m between each on the Nile Delta.¹ Future plans include mapping out a larger region for bigger sample size and showing if there is variation in the concentration of monazite near the Mississippi River.

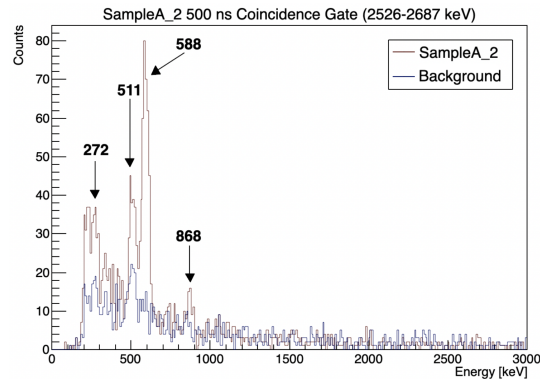


FIGURE 9: Sample A 1-D projection to Y-axis of the ^{232}Th (2614 keV) coincidence gate. The labeled peaks correspond to transitions from Fig. 4 (^{208}Pb).

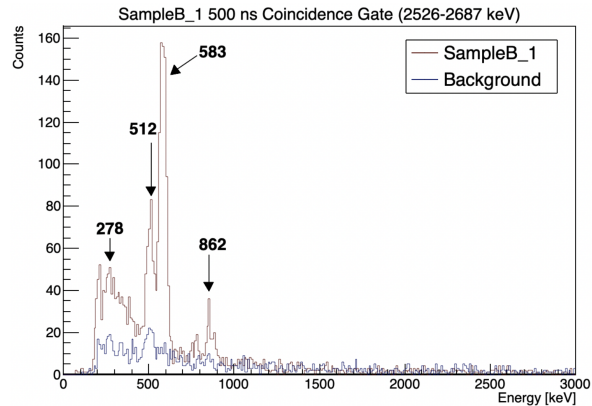


FIGURE 10: Sample B 1-D projection to Y-axis of the ^{232}Th (2614 keV) coincidence gate. The labeled peaks correspond to transitions from Fig. 4 (^{208}Pb).

ACKNOWLEDGMENTS

We would like to thank Keith Frye, Adian Edmondson, Ashley Ip, and Sabid Hossain for their contributions to the experimental setup. We would also like to thank Ronald Unz for the collection and preservation of samples from the Great River Road State Park.

REFERENCES

1. F. Mubarak, M. Fayez-Hassan, N. A. Mansour, T. S. Ahmed, and A. Ali, *Sci. Rep.* **7** (2017).
2. J. Santos, H. Conceicao, M. Leandro, and M. Rosa, *Braz. J. Geol.* **48**, 721–733 (2018).
3. J. Mertie, Jr., “Monazite placers in the Southeastern Atlantic states,” *Geological Survey Bulletin* 1390 (1975).
4. A. Bicker, Jr., “Economic minerals of Mississippi,” *Mississippi Geological Economic and Topographical Survey* (1970).
5. V. Vineethkumar, R. Akhil, K. P. Shimod, and V. Prakash, *J. Radioanal. Nucl. Chem.* **327**, 1–10 (2021).
6. Rene Brun and Fons Rademakers, *Proceedings AIHENP’96 Workshop*, Lausanne, Sept. 1996.
7. A. Tillett, L. Benninger, J. Dermigny, and C. Iliadis, *Appl. Radiat. Isot.* **141**, 24–32 (2018).
8. A. Tillett, J. Dermigny, M. Emamian, Y. Tonin, I. Bucay, R. L. Smith, M. Darken, C. Dearing, M. Orbon, and C. Iliadis, *Nucl. Instrum. Methods Phys. Res., Sect. A* **871**, 66–71 (2017).